Polymer 50 (2009) 5970–5979

Contents lists available at ScienceDirect

Polymer

journal homepage: www.elsevier.com/locate/polymer

# Synthesis of hollow polymer microspheres with movable polyelectrolyte core and functional groups on the shell-layer

Min Ji, Bin Liu, Xinlin Yang*, Junyou Wang

*Key Laboratory of Functional Polymer Materials, The Ministry of Education, Institute of Polymer Chemistry, Nankai University, Tianjin 300071, China*

ARTICLE INFO

*Article history:*
Received 20 May 2009
Received in revised form
21 October 2009
Accepted 27 October 2009
Available online 31 October 2009

*Keywords:*
Hollow polymer microspheres
Movable polyelectrolyte core
Distillation precipitation polymerization

ABSTRACT

Hollow polymer microspheres with movable quaternary pyridinium polyelectrolyte (PE) cores and various functional groups on the shell-layers, such as hydroxyl, amide, and carboxyl, were prepared by the selectively etching of mid-silica layer with hydrofluoric acid from the corresponding poly(ethyleneglycol dimethacrylate-*co*-methacrylic acid)@poly(ethyleneglycol dimethacrylate- *co*-4-vinylpyridinium benzylchloride)/silica/polymer (P(EGDMA-*co*-MAA) @P(EGDMA-*co*-VPyBzCl)/$SiO_2$/polymer) tetra-layer microspheres. The tetra-layer hybrid microspheres were synthesized by a multi-stage reaction process, which included the combination of distillation precipitation polymerization for the formation of polymer-layers and the hydrolysis of tetraethyl orthosilicate (TEOS) via a modified Stöber sol–gel procedure to afford silica layer. The efficient electrostatic interaction between the cationic pyridinium species on the surface of P(EGDMA-*co*-MAA)@P(EGDMA-*co*-VPyBzCl) cores and the negative charges on the silica species was essential to get monodisperse tri-layer P(EGDMA-*co*-MAA)@P(EGDMA-*co*-VPyBzCl)/$SiO_2$ microspheres during the hydrolysis of TEOS. The functional polymer shell was encapsulated over 3-(methacryloxy)propyl trimethacrylate (MPS) modified tri-layer polymer/silica seeds by distillation precipitation copolymerizations of *N*,*N*′-methylenebisacrylamide (MBAAm) crosslinker and comonomers with different functional groups, including *N*-isopropylacrylamide (NIPAAm), 2-hydroxyethylmethacrylate (HEMA) and methacrylic acid (MAA), with 2,2′-azobisisobutyronitrile (AIBN) as an initiator in neat acetonitrile. The morphology and structure of the tetra-layer hybrid microspheres and the corresponding hollow microspheres with movable PE core and functional polymer shell-layer were characterized by transmission electron microscopy (TEM), Fourier-transform infrared spectroscopy (FT-IR), ξ-potential, and dynamic light scattering (DLS).

## 1. Introduction

In recent years, hollow polymer microspheres have attracted much attention due to their wide applications, including the encapsulation for controlled-release of drugs and enzymes, fillers, catalysts, and adsorption materials for sound [1–5]. A variety of physical and chemical techniques have been reported for the preparation of hollow polymer microspheres such as the encapsulation of a hydrocarbon non-solvent [6], micelle formation of block copolymers with subsequent shell-crosslinking and degradation of the core [7], surface-initiated atom transfer radical polymerization (ATRP) [8], polycondensation interfacial polymerization [9,10], and layer-by-layer deposition of polyelectrolyte onto sacrificial templates [11–13].

Hollow polymer microspheres have some excellent properties, such as low density, high specific area, good flow ability, and surface permeability. Especially, their big cavities can encapsulate functional nanoparticles as cores. This interesting structure with novel functionalities is different from those of the host hollow microspheres and the guest nanoparticles. There have been two ways to acquire hollow polymer microspheres with movable cores. One is based on a template-assisted approach for the synthesis of polymer microspheres having tri-layer structures with subsequently selective removal of the sacrificial mid-layer. Different nanoparticles, such as gold [14,15], silver [16], tin [17], silica [18,19], polymer beads [20,21], and iron oxides [22–24] have been encapsulated into the interior of different hollow particles as movable cores via different techniques. The other is the in-situ synthesis of the movable nanocolloid-cores inside the cavity of the preformed hollow polymer microspheres [25,26]. Monodispersity and various polarity with different functional groups on the shell-layer of the hollow polymer microspheres are important to improve their performance and functionality for many applications, such as for

---

* Corresponding author. Tel.: +86 22 23502023; fax: +86 22 23503510.
*E-mail address:* xlyang88@nankai.edu.cn (X. Yang).

0032-3861/$ – see front matter © 2009 Elsevier Ltd. All rights reserved.
doi:10.1016/j.polymer.2009.10.063

a micro-reactor containing gold nanoparticles inside as a catalyst [27]. The interaction of microparticles with biological cells depends on the size, size distribution and functionality of the particles [28]. If the size distribution of microparticles is narrower, physical and chemical properties are more uniform, thereby making it easier, for example, to formulate more sophisticated drug deliver system [29]. It is much difficult for both dispersion polymerization and emulsion polymerization to control the size and size distribution of either the hollow spheres or hollow spheres with movable cores.

Polyelectrolytes (PEs) are often used to modify the surface properties of various materials and have potential applications in many fields, such as contact lens, modification of surfaces of titanium implants, wound dressings for serious burns, separation membranes for gases and dissolved species [30–33].

In our previous works, monodisperse silica/polymer core–shell microspheres and the corresponding hollow microspheres with various polarity and functional groups on the shell-layer were prepared by distillation precipitation polymerization [34–37]. In these works, the size and size distribution of the hollow polymer microspheres can be well controlled during the polymerization in absence of any stabilizer or surfactant and the various functional groups can be incorporated into the polymer shell-layer. In the present work, we describe a facile method for the synthesis of hollow polymer microspheres with different functional groups, such as amide, hydroxyl, and carboxyl, containing movable polyelectrolyte cores. The present method offers an alternative approach to the synthesis of monodisperse hollow polymer microspheres having different functional groups and movable cores.

## 2. Experimental

### 2.1. Chemicals

Tetraethyl orthosilicate ($Si(OEt)_4$, TEOS), *N*-isopropylacrylamide (NIPAAm) and ethyleneglycoldimethacrylate (EGDMA) were purchased from Aldrich and used without any further purification. 3-(Methacryloxy)porpyl trimethoxysilane (MPS) was available from Aldrich and distilled under vacuum. *N*,*N*′-Methylenebisacrylamide (MBAAm, chemical grade, Tianjin Bodi Chemical Engineering Co.) was recrystallized from acetone. Methacrylic acid (MAA) and 2-hydroxyethyl methacrylate (HEMA) were provided by Tianjin Chemical Reagent II Co. and 4-vinylpyridine (VPy) was obtained from Alfa Aesar. All these functional comonomers were purified by vacuum distillation. 2,2′-Azobisisobutyronitrile (AIBN) was got from Chemical Factory of Nankai University and recrystallized from methanol. Acetonitrile (analytical grade, Tianjin Chemical Reagent II Co.) was dried over calcium hydride and purified by distillation before use. Hydrofluoric acid (HF, containing 40% of HF was available from Tianjin Chemical Reagent Institute). All the other reagents, including benzyl chloride (BzCl, Tianjin Chemical Reagent II Co.), were analytical grade and used without any further treatment.

### 2.2. Synthesis of monodisperse P(EGDMA-co-MAA)@P(EGDMA-co-VPyBzCl) polyelectrolyte microspheres

The preparation of poly(ethyleneglycol dimethacrylate-*co*-methacrylic acid) (P(EGDMA-*co*-MAA)) microspheres by first-stage distillation precipitation polymerization was reported in detail by our previous work [38], in which the EGDMA crosslinking degree was 0.20 (as mass ratio) and AIBN was used as the initiator. The loading capacity of the accessible carboxyl groups on the surface of P(EGDMA-*co*-MAA) microspheres was 4.00 mmol/g as determined by acid–base titration. P(EGDMA-*co*-MAA)@poly(ethyleneglycol dimethacrylate-*co*-4-vinyl pyridine) (P(EGDMA-*co*-MAA)@-P(EGDMA-*co*-VPy)) core–shell microspheres were synthesized by the second-stage distillation precipitation polymerization, in which the formation of core–shell structure was driven by the efficient hydrogen-bonding interaction between the carboxyl group and pyridyl group of VPy as described in our previous work [39]. The loading capacity of the accessible pyridyl group on the surface of P(EGDMA-*co*-MAA)@P(EGDMA-*co*-VPy) microspheres was 1.91 mmol/g as determined by the acid–base titration.

Monodisperse P(EGDMA-*co*-MAA)@ poly(ethyleneglycol dimethacrylate-*co*-4-vinyl pyridinium benzyl chloride) (P(EGDMA-*co*-MAA)@P(EGDMA-*co*-VPyBzCl)) cationic (PE) microspheres were synthesized as following: 0.5 g of P(EGDMA-*co*-MAA)@P(EGDMA-*co*-VPy) microspheres (containing 0.95 mmol of –Py) were immersed in 80 mL of BzCl solution in dimethylformamide (DMF, containing 0.28 g, 2.2 mmol BzCl). The quaternary pyridinium reaction was carried out at 60 °C for 24 h. After the reaction, the resultant cationic PE microspheres were separated by vacuum filtration over a G-5 sintered glass filter and successively washed with ethanol for three times. The cationic polymer microspheres were dried in vacuum oven at 50 °C till constant weight.

### 2.3. Preparation of MPS-modified PE/$SiO_2$ composite microspheres

PE/$SiO_2$ tri-layer microspheres were synthesized by coating of an outer layer of silica onto PE nanoparticles via a modified Stöber sol–gel process. About 0.05 g of quaternary pyridinium PE nanoparticles, 0.50 mL of TEOS and 1.20 mL ammonia were consecutively added into a water/ethanol (10/80 mL) mixture with vigorous stirring. The sol–gel process was allowed to proceed for 12 h to obtain the pyridinium PE/$SiO_2$ composite microspheres.

Modification of PE/$SiO_2$ composite microspheres with MPS to incorporate the reactive vinyl groups was achieved by introducing MPS (2.0 mL) into the above water/ethanol suspension of composite particles under stirring and the reaction mixture was stirred further for 48 h at room temperature. The resultant MPS-modified PE/$SiO_2$ composite microspheres were purified by centrifugation, decantation and resuspension in ethanol for three cycles to remove the excessive MPS. The final MPS-modified PE/$SiO_2$ composite microspheres were dried in a vacuum oven at 50 °C till constant weight.

### 2.4. Preparation of pyridinium PE/$SiO_2$/polymer hybrid microspheres with functional groups on the shell-layer

A typical procedure for the distillation precipitation copolymerization in the presence of MPS-modified pyridinium PE/$SiO_2$ microspheres as seeds was as following: In a dried 50 mL of two-necked flask, 0.10 g of MPS-modified PE/$SiO_2$ seeds were suspended in 40 mL of acetonitrile as an ivory-white suspension. Then MBAAm (0.06 g, 0.39 mmol) crosslinker, NIPAAm (0.09 g, 0.80 mmol) and AIBN (0.005 g, about 2 wt% relative to the total comonomers) were dissolved in the suspension. The two-necked flask attaching with a fractionating column, Liebig condenser, and receiver was submerged in a heating mantle. The reaction mixture was heated from ambient temperature till the boiling state within 8 min and the reaction system was kept under the refluxing state for a further 22 min. The polymerization was ended after 20 mL of acetonitrile was distilled off the reaction system within 75 min. After the polymerization, the resultant PE/$SiO_2$/poly(*N*,*N*′-methylenebisacryl amide-*co*-*N*-isopropyl acrylamide) (PE/$SiO_2$/P(MBAAm-*co*-NIPAAm)) tetra-layer hybrid microspheres were purified by repeating centrifugation, decantation, and resuspension in acetone with ultrasonic irradiation for three times. The resultant tetra-layer hybrid microspheres were then dried in a vacuum oven at 50 °C till constant weight.

A series of synthesis using different functional comonomers, including HEMA and MAA, respectively, together with a MBAAm crosslinker, were performed by distillation precipitation copolymerization in the presence of MPS-modified PE/$SiO_2$ as seeds to afford the PE/$SiO_2$/polymer hybrid microspheres with various functional groups on the outer polymer shell-layer, while MBAAm crosslinking degree in the comonomer feed was maintained at 0.40 as mass ratio and AIBN was kept at 2 wt% corresponding to the total comonomers. The treatment of these PE/$SiO_2$/polymer hybrid microspheres with hydroxyl and carboxyl groups on the shell-layer was the same as that of the typical procedure for PE/$SiO_2$/P(MBAAm-*co*-NIPAAm) tetra-layer hybrid.

The above afforded PE/$SiO_2$/polymer hybrid microspheres with hydroxyl and carboxyl groups on the shell-layer were used as seeds for the multi-semibatch distillation precipitation polymerization. For the second aliquot of the polymerization, a mixture of 0.06 g of MBAAm crosslinker together with 0.09 of either HEMA or MAA comonomers and 0.003 g of AIBN initiator in 80 mL of acetonitrile was added to the residual reaction system after the first cycle copolymerization. The polymerization was continued under the same conditions as the first aliquot. The final PE/$SiO_2$/polymer tetra-layer microspheres with thicker polymer shell-layers were treated by the same procedure as above hybrids.

The reproducibility of the distillation precipitation polymerization for the synthesis of these hybrid microspheres containing various functional groups was confirmed by several duplicate and triplicate experiments.

### 2.5. *Preparation of hollow polymer microspheres with movable PE cores and functional groups on the shell-layer*

The resultant pyridinium PE/$SiO_2$/polymer tetra-layer hybrid microspheres were immersed in 40 wt% HF solution under low frequency oscillating at room temperature for 6 h. The excessive HF and the formed $SiF_4$ gas were expelled out of the reaction system by vacuum filtration over a G-5 sintered glass filter. The hollow polymer microspheres with movable pyridinium PE cores and various functional groups on the shell-layer, including amide, hydroxyl and carboxyl, were purified by several centrifugation/washing cycles in water till the pH of the solution at 7. The resultant hollow polymer particles were then dried in a vacuum oven at 50 °C till constant weight.

### 2.6. *Characterization*

The morphology, size and size distribution P(EGDMA-*co*-MAA), P(EGDMA-*co*-MAA)@P(EGDMA-*co*-VPy), pyridinium polyelectrolyte microspheres (PE), pyridinium PE/$SiO_2$, PE/$SiO_2$/polymer microspheres with various functional groups on the shell-layer and the corresponding hollow polymer microspheres with movable PE cores were determined by transmission electron microscopy (TEM, Tecnai G2 20S-TWIN). All the size and size distribution reflect the averages about 100 particles each, which are calculated according to the following formula:

$$U = D_w/D_n \quad D_n = \sum_{i=1}^{k} n_i D_i \Big/ \sum_{i=1}^{k} n_i \quad D_w = \sum_{i=1}^{k} n_i D_i^4 \Big/ \sum_{i=1}^{k} n_i D_i^3$$

where $U$ is the polydispersity index, $D_n$ is the number-average diameter, $D_w$ is the weight-average diameter, $N$ is the total number of the measured particles, and $D_i$ is the particle diameters of the determined microparticles.

Fourier-transform infrared spectra (FT-IR) were scanned over the range of 400–4000 $cm^{-1}$ with potassium bromide plate on a Bio-Rad FTS135 FT-IR spectrometer.

The zeta-potential was determined with Zeta Pals (Brookhaven Instrument Cooperation) by measuring the electrophoretic mobility of the particles using anhydrous ethanol as the electrolyte. The concentration of the polyelectrolyte suspension was about 0.001 mg/mL at room temperature.

The hydrodynamic diameters of the hollow polymer microspheres with movable PE cores and various functional groups on the shell-layer were measured by dynamic light scattering (DLS) on a laser light scattering spectrometer (BI-200 SM) equipped with a Brookhaven BI-9000 AT digital correlator and a He–Ne laser at 659 nm. All the samples were measured at 25 °C with the scattering angle of 90°.

## 3. Results and discussion

Scheme 1 described the synthesis of pyridinium PE/$SiO_2$/polymer tetra-layer microspheres via a four-stage reaction and the further development of corresponding hollow polymer microspheres with movable PE cores and various functional groups on the polymer shell-layers, such as amide, hydroxyl, and carboxyl. Such procedures mainly included the distillation precipitation polymerization to afford the inner P(EGDMA-*co*-MAA)@P(EGDMA-*co*-VPy) core and polymer outer shell-layer with functional groups, and the controlled hydrolysis of TEOS in water/ethanol mixed solvent to get inorganic silica mid-layer, and the final formation of the hollow polymer microspheres with movable PE cores and functional groups on the shell-layer via the selective removal of the sandwiched silica-layer with hydrofluoric acid.

### 3.1. *Synthesis of quaternary pyridinium cationic polymer microspheres*

To get monodisperse polymer microspheres with pyridyl groups on the surface, two-stage distillation precipitation polymerizations were used and the typical TEM micrographs of the resultant polymer microspheres were shown in Fig. 1A and B, respectively. The results indicated that P(EGDMA-*co*-MAA) (Fig. 1A) and P(EGDMA-*co*-MAA)@P(EGDMA-*co*-VPy) (Fig. 1B) core–shell microspheres had spherical shape with smooth surface. The average diameter of P(EGDMA-*co*-MAA) microsphere was 235 nm and a narrow-dispersity index ($U$) of 1.013 as summarized in Table 1. The loading capacity of the accessible carboxyl groups on the surface of P(EGDMA-*co*-MAA) microsphere was 4.00 mmol/g with crosslinking degree of 0.20, which were used as seeds for the second-stage distillation precipitation polymerization to afford monodisperse P(EGDMA-*co*-MAA)@P(EGDMA-*co*-VPy) core–shell microspheres via the efficient hydrogen-bonding interaction between the carboxyl groups and the pyridyl groups as illustrated in Scheme 1. The hydrogen-bonding interaction between the carboxyl group and pyridyl group acted as a driving force for the construction of core–shell polymer microspheres [39] and the growth of polymer microspheres [40] have been investigated in detail by our previous works. The size of the P(EGDMA-*co*-MAA)@P(EGDMA-*co*-VPy) core–shell microspheres as tabulated in Table 1 was 247 nm with a narrow-dispersity index ($U$) of 1.020. This meant that the thickness of P(EGDMA-*co*-VPy) shell-layer was about 6 nm, which was calculated as half of the difference between the diameter of P(EGDMA-*co*-MAA) core and that of core–shell microspheres. The loading capacity of the accessible pyridyl group on the surface of the core–shell microspheres was 1.91 mmol/g determined by the acid–base titration. Both of the P(EGDMA-*co*-MAA) and P(EGDMA-*co*-MAA)@P(EGDMA-*co*-VPy) microspheres

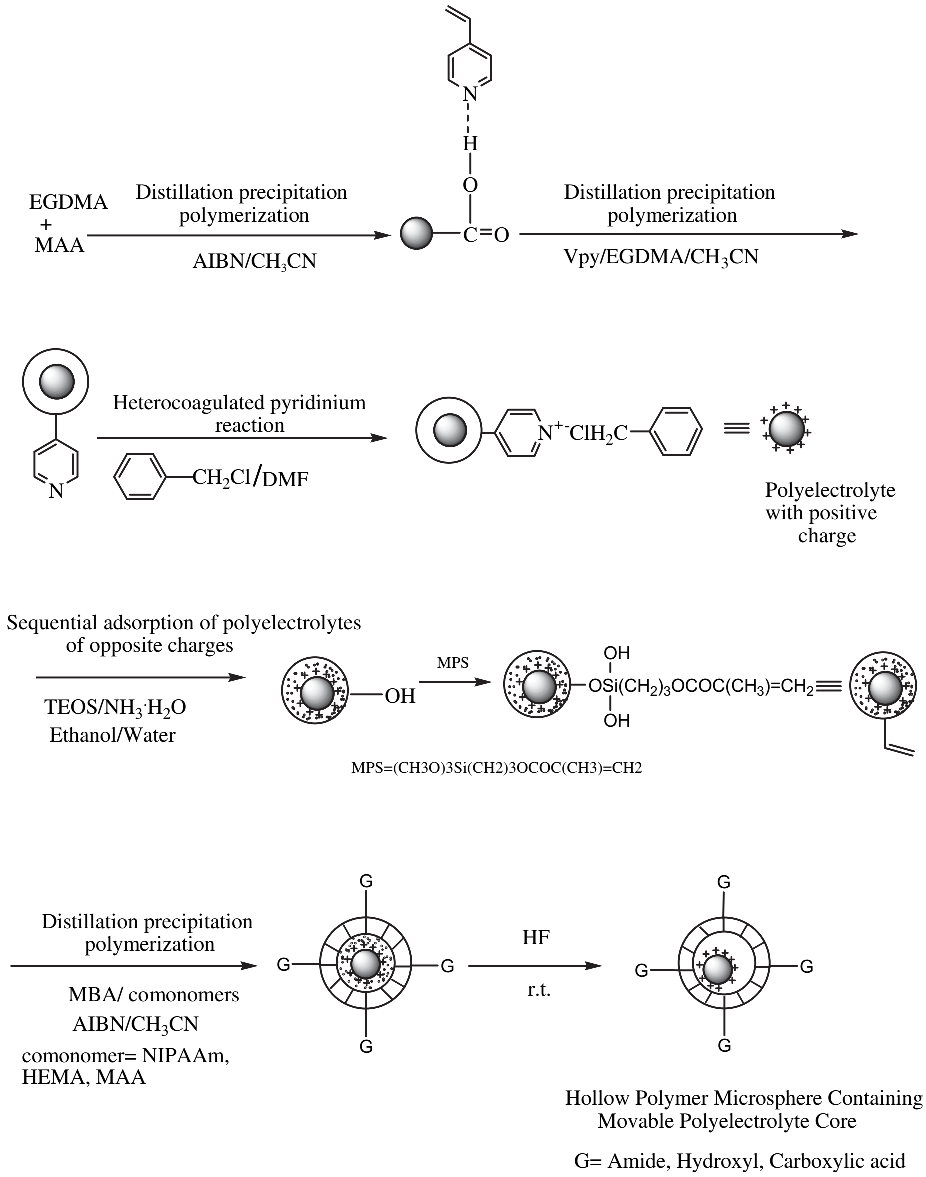

**Scheme 1.** Preparation of hollow polymer microspheres with movable polyelectrolyte cores and various functional groups on the shell-layer.

occurred as a duplet or multiplet particles in TEM micrographs in Fig. 1A and B, which may be due to the strong inter-particle hydrogen-bonding interaction and soft surface of the polymer microspheres in the case of low crosslinking degree. For both the P(EGDMA-*co*-MAA) and P(EGDMA-*co*-MAA)@P(EGDMA-*co*-VPy) microspheres, the FT-IR spectra in Fig. 2a and b had a strong peak at 1731 $cm^{-1}$ corresponding to the characteristic stretching vibration of the carbonyl component of the ester group. Comparing to the FT-IR spectrum of P(EGDMA-*co*-MAA) core in Fig. 2a, the FT-IR spectrum of P(EGDMA-*co*-MAA)@P(EGDMA-*co*-VPy) microspheres in Fig. 2b behaved a new peak at 1597 $cm^{-1}$ assigning to the typical vibration of the pyridyl group.

The TEM micrograph of P(EGDMA-*co*-MAA)@P(EGDMA-*co*-VPyBzCl) cationic (PE) microspheres in Fig. 1C indicated that the polyelectrolyte particles maintained the spherical shape and smooth surface during the quaternary pyridinium modification of the pyridyl group with benzyl chloride (BzCl), while the average size of the pyridinium particles was kept at 247 nm and a monodispersity index ($U$) of 1.008 as summarized in Table 1. This implied that all the polymer microspheres were physically stable and remained monodispersion during the pyridinium process. The well-separated cationic PE particles with smooth surface in Fig. 1C were originated from the strong inter-particle electrostatic repulsion. This was much different from the observation of P(EGDMA-*co*-MAA) and P(EGDMA-*co*-MAA)@P(EGDMA-*co*-VPy) microspheres in Fig. 1A and B, in which the dimmer and trimer particles were observed due to the inter-particle hydrogen-bonding interaction.

The successful quaternary pyridinium modification of the P(EGDMA-*co*-MAA)@P(EGDMA-*co*-VPy) microspheres was confirmed further by the FT-IR spectra in Fig. 2c with disappearance of the peak at 1597 $cm^{-1}$ corresponding to the stretching vibration of pyridyl group and the presence of a new peak at 1619 $cm^{-1}$ assigning to the stretching vibration of the quaternary pyridinium group of PE particles. The zeta-potential of cationic PE microspheres was +34.55 mV determined by a zeta-potential analysis as summarized in Table 1, while the zeta-potential of P(EGDMA-*co*-MAA)@P(EGDMA-*co*-VPy) microspheres was −7.05 mV. In a word, the pyridyl group of P(EGDMA-*co*-MAA)@P(EGDMA-*co*-VPy) microspheres were quantitatively converted to the corresponding quaternary pyridinium group of PE microspheres via such efficient

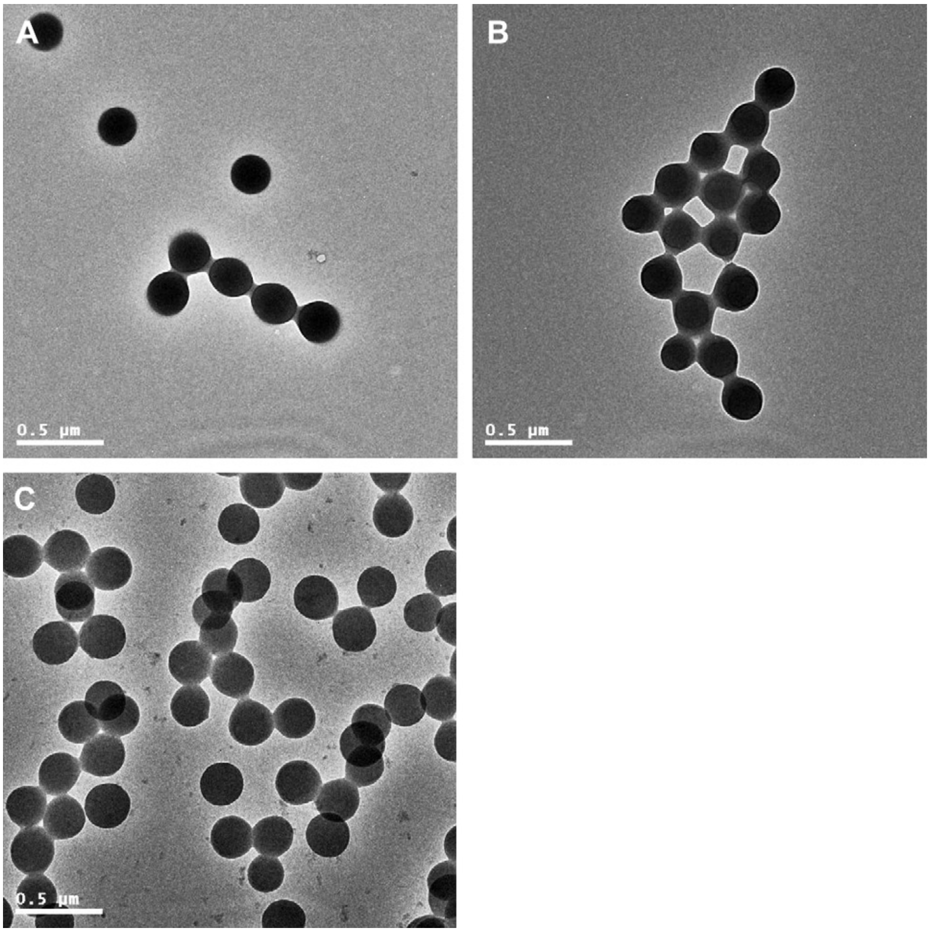

**Fig. 1.** TEM micrographs: (A) P(EGDMA-*co*-MAA); (B) P(EGDMA-*co*-MAA)@P(EGDMA-*co*-Vpy); (C) Quaternary pyridinium P(EGDMA-*co*-MAA)@P(EGDMA-*co*-VpyBzCl).

modification, which permitted the further coating of silica layer via a modified Stöber sol–gel process over the PE microspheres.

### *3.2. Synthesis of MPS-modified PE/SiO$_2$ composite microspheres*

Composite copolymer-silica particles with well-defined core–shell morphologies were formed via the confined deposition of silica species over the partially quaternary cationic poly(2-(dimethyl amino)ethyl methacrylate) (PDMA) and hydrophobic poly(2-(diisopropylamino)ethyl methacrylate) (PDPA) cores [41]. The Stöber method has been adopted to prepare polymer/silica core–shell particles by coating the surfaces of the monodisperse polystyrene (PSt) beads with uniform silica shells in the pH range of 10–12 to balance the nucleation and growth of silica sols [42]. Stable PSt/SiO$_2$ composite core–shell colloids with PSt as core and silica as shell were synthesized via a surfactant-free process by the hydrolysis and condensation of TEOS in acidic aqueous ethanol medium in the presence of cationic PSt colloids as seeds [43]. Monodisperse P(EGDMA-*co*-MAA)/SiO$_2$ microspheres were prepared by coating of a layer of silica onto P(EGDMA-*co*-MAA) cores via sol–gel process with the aid of the hydrogen-bonding interaction between the carboxyl group on the surface of polymer cores and the hydroxyl groups of silica species [22]. In the present work, pyridinium PE cationic particles were uniformly coated with silica shell via the sol–gel hydrolysis of TEOS with aqueous ammonia as a catalyst. Here, the electrostatic interaction between the cationic pyridinium PE cores and the negative charges of the silica species played an essential role during the hydrolysis for building the PE/SiO$_2$ composite microspheres as shown in Scheme 1. The TEM micrograph of PE/SiO$_2$ in Fig. 3A indicated that uniform coating of silica onto cationic pyridinium PE cores was only formed with smooth surface in absence of any secondary-silica particles, in which as typical core–shell structure was clearly observed with a lighter contrast of PE cores and a deeper contrast of silica shell-layers. The essential role of the quaternary pyridinium groups on the surface of the cationic PE cores was confirmed further by the formation of P(EGDMA-*co*-MAA)@-P(EGDMA-*co*-VPy)/SiO$_2$ composite microspheres with rough surfaces in Fig. 3B of TEM micrograph, although the hydrogen-bonding interaction between the pyridyl group on the surface of the polymer cores and the hydroxyl groups of the silica species was present during the hydrolysis of TEOS. Raspberry-like P(EGDMA-*co*-VPy)/SiO$_2$ core–corona composites were prepared by a self-assemble heterocoagulation based on a hydrogen-bonding interaction between the pyridyl group of P(EGDMA-*co*-VPy) core and the hydroxyl group of silica corona in our previous work [44].

**Table 1**
The size, size distribution and zeta-potential of polymer microspheres.

| Entry | $D_n$ (nm) | $D_w$ (*nm*) | $U$ | Thickness of outer layer | Zeta-potential (vm) |
|---|---|---|---|---|---|
| A | 235 | 238 | 1.013 | 0 | – |
| B | 247 | 252 | 1.020 | 6 | −7.05 |
| C | 247 | 249 | 1.008 | 6 | 34.55 |
| D | 404 | 406 | 1.005 | 78.5 | −57.1 |
| E | 405 | 407 | 1.006 | 79 | – |

(A) P(EGDMA-*co*-MAA); (B) P(EGDMA-*co*-MAA)@P(EGDMA-*co*-Vpy); (C) Pyridinium P(EGDMA-*co*-MAA)@P(EGDMA-*co*-VpyBzCl) (PE); (D) PE/SiO$_2$; (E) MPS-modified PE/SiO$_2$.

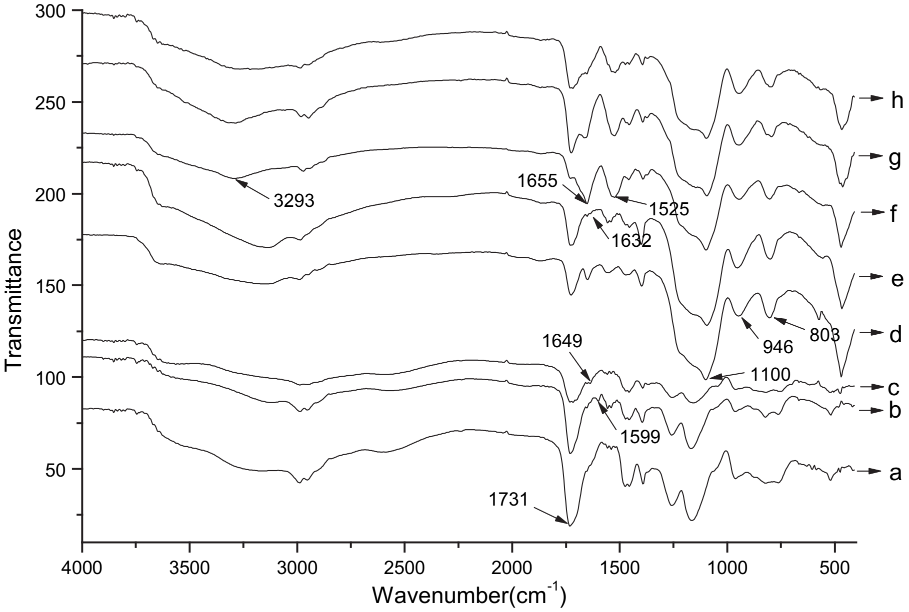

**Fig. 2.** FT-IR spectra of polymer microspheres: (a) P(EGDMA-*co*-MAA); (b) P(EGDMA-*co*-MAA)@P(EGDMA-*co*-Vpy); (c) Quaternary pyridinium P(EGDMA-*co*-MAA)@P(EGDMA-*co*-VpyBzCl) (PE); (d) PE/$SiO_2$; (e) MPS-modified PE/$SiO_2$; (f) PE/$SiO_2$/P(MBAAm-*co*-NIPAAm); (g) PE/$SiO_2$/P(MBAAm-*co*-HEMA); (h) PE/$SiO_2$/P(MBAAm-*co*-MAA).

The particle size of PE/$SiO_2$ composite was significantly increased from 247 nm of PE core to 404 nm with a monodispersity index ($U$) of 1.005 as summarized in Table 1. In other words, the thickness of the silica shell-layer was 78 nm via coating of the pyridium PE cores during the third-stage sol–gel hydrolysis of TEOS with the aid of the electrostatic interaction.

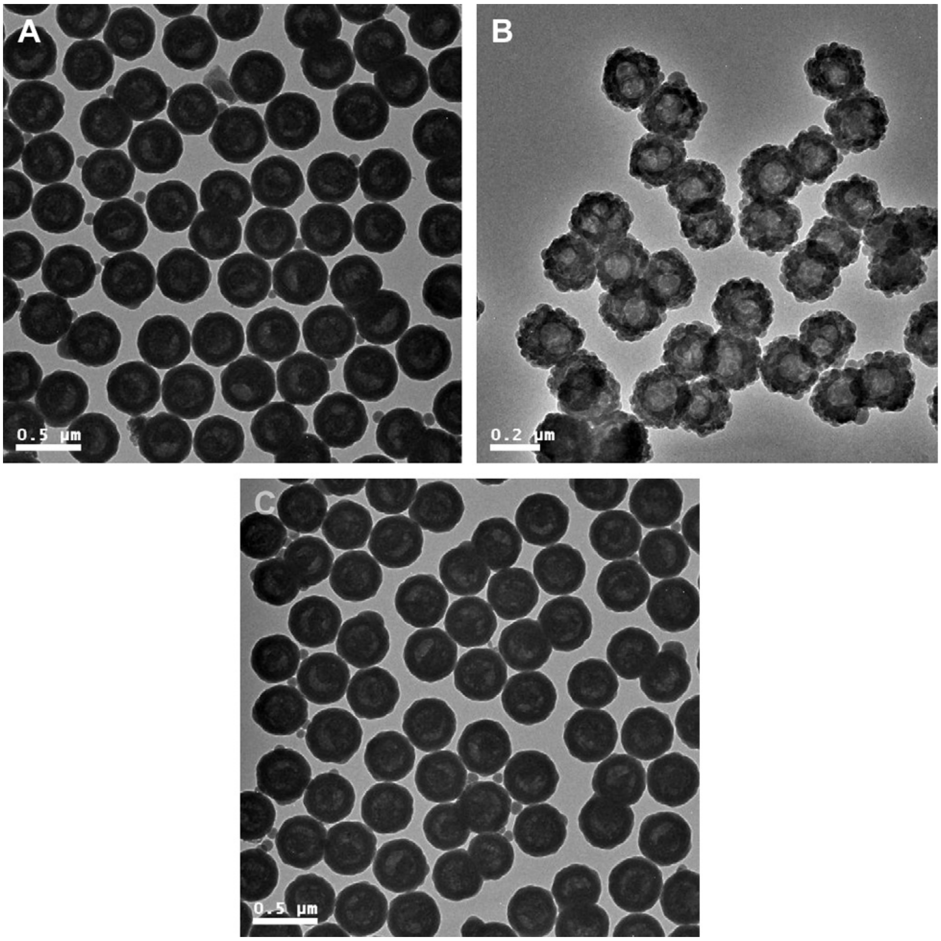

**Fig. 3.** TEM micrographs: (A) PE/$SiO_2$; (B) P(EGDMA-*co*-MAA)@P(EGDMA-*co*-Vpy)/$SiO_2$; (C) MPS-modified PE/$SiO_2$.

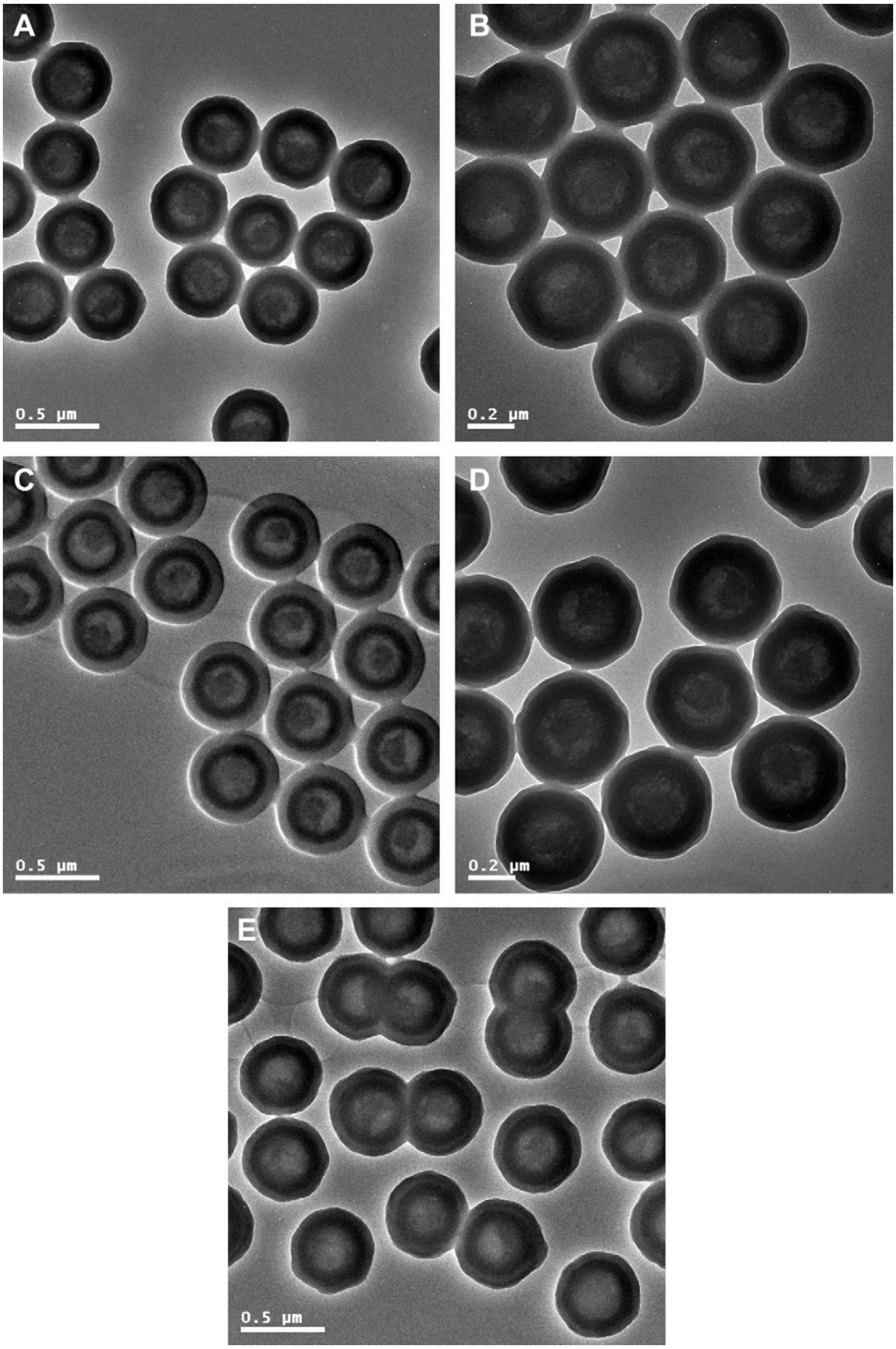

**Fig. 4.** TEM micrographs: (A) PE/$SiO_2$/P(MBAAm-*co*-NIPAAm); (B) PE/$SiO_2$/P(MBAAm-*co*-HEMA) after first-semibatch polymerization; (C) PE/$SiO_2$/P(MBAAm-*co*-HEMA) after second semibatch polymerization; (D) PE/$SiO_2$/P(MBAAm-*co*-MAA) after first-semibatch polymerization; (E) PE/$SiO_2$/P(MBAAm-*co*-MAA) after second semibatch polymerization.

The successful encapsulation of the silica layer over the pyridinium PE core was confirmed by FT-IR spectra as illustrated in Fig. 2. The FT-IR spectrum in Fig. 2d of PE/$SiO_2$ composite particles had the strong peaks at 1100, 946 and 803 $cm^{-1}$ corresponding to the characteristic absorption of the Si–O–Si bond of the silica shell-layer. The successful synthesis of the PE/$SiO_2$ composites was proven further by the zeta-potential value of $-57.1$ mV as summarized in Table 1, which were much different from those of P(EGDMA-*co*-MAA)@P(EGDMA-*co*-VPy) core–shell microspheres ($-7.05$ mV) and the cationic pyridinium PE cores ($+34.55$ mV), respectively. These results suggested that the negative surface charge of PE/$SiO_2$ composites were fully covered with silica shell-layer onto PE cores via the controlled hydrolysis of TEOS in water/ethanol mixed solvent with aqueous ammonia as catalyst.

The residual vinyl groups on the surface of poly(divinylbenzene) (PDVB) microspheres were essential to the growth of polymer microspheres for distillation precipitation polymerization [45], during which the newly formed oligomer radicals and monomers were captured by these reactive vinyl groups. Monodisperse MPS-modified PE/$SiO_2$ microspheres were prepared by the hydrolysis of MPS via the self-condensation reaction of the hydroxyl groups for siliceous species to incorporate the reactive vinyl groups on the surface of composite particles, which was much similar to the modification process in the literature [46]. The TEM micrograph of MPS-modified PE/$SiO_2$ microspheres as shown in Fig. 3C indicated that these particles had spherical shape and smooth surface with an average diameter of 405 nm and monodispersity index ($U$) of 1.012 as summarized in Table 1, which implied that only a very thin siliceous layer was formed during the modification of MPS in order to incorporate the reactive vinyl groups onto the surface of PE/$SiO_2$ composite microspheres. The FT-IR spectrum of MPS-modified PE/$SiO_2$ microspheres in Fig. 2e displayed a new peak at 1632 $cm^{-1}$ corresponding to the characteristic stretching vibration of the vinyl group from MPS component, which permitted the further growth of the PE/$SiO_2$ particles to result in PE/$SiO_2$/polymer tetra-layer microspheres with different functional groups on the outer polymer shell-layer via the further stage distillation precipitation polymerization.

### *3.3. Synthesis of monodisperse PE/$SiO_2$/Polymer tetra-layer microspheres with various functional groups on the shell-layer*

Polymer microspheres with various functional groups have many applications in different fields, such as carriers for the immobilization of biological substances including enzymes, antibodies, etc [47,48]. The typical TEM micrograph of PE/$SiO_2$/P(MBAAm-*co*-NIPAAm) microspheres with MBAAm crosslinking degree of 40% (mass ratio) was illustrated in Fig. 4A with a multi-layer structure: a lighter contrast of PE core and P(MBAAm-*co*-NIPAAm) shell-layer and a deep contrast of sandwiched silica-layer. It revealed that the hybrid microspheres had spherical shape and smooth surface, which was much different from the results of the rough surfaces for $SiO_2$/PMBAAm core–shell composites due to the high reactivity of MBAAm crosslinker in our previous work [34]. The FT-IR spectrum of PE/$SiO_2$/P(MBAAm-*co*-NIPAAm) microspheres in Fig. 2f behaved the strong peaks at 3293, 1655, and 1525 $cm^{-1}$ assigning to the stretching vibration of *N–H* bond, carbonyl component of amide group, and the bending vibration of *N–H* bond of P(MBAAm-*co*-NIPAAm) shell-layer, respectively.

To investigate whether the other functional groups can be incorporated onto the outer polymer shell-layer of the PE/$SiO_2$/polymer hybrids by altering the kind of functional comonomers including HEMA and MAA, respectively, were copolymerized with an MBAAm crosslinker (40% of crosslinking degree as mass ratio in the comonomer feed) in the presence of MPS-modified PE/$SiO_2$ particles as seeds. The TEM micrographs of the resultant PE/$SiO_2$/P(MBAAm-*co*-HEMA) and PE/$SiO_2$/P(MBAAm-*co*-MAA) hybrids were shown in Fig. 4B and D, respectively. The results indicated that the PE/$SiO_2$/polymer hybrids with different functional groups, such as hydroxyl (Fig. 4B) and carboxyl (Fig. 4D) had spherical shape with smooth surface, in which the multi-layer structure of the hybrids was clearly observed with a light contrast PE core and polymer outer shell-layer together in presence of a deep contrast of sandwiched silica-layer.

The main purpose of the present work was to introduce the functional groups during the fourth-stage distillation precipitation polymerization and to retain the particle monodispersity in absence of the secondary-initiated polymer particles. A series of monodisperse PE/$SiO_2$/P(MBAAm-*co*-HEMA) and PE/$SiO_2$/P(MBAAm-*co*-MAA) hybrids with different shell-thicknesses of outer polymer shell-layers were prepared by a multi-semibatch polymerization mode. The typical TEM micrographs of these hybrid microspheres were shown in Fig. 4C (hydroxyl group) and Fig. 4E (carboxyl), respectively. Both TEM micrographs (Fig. 4C and E) demonstrated that the final hybrid microspheres had spherical and smooth surface with a significant thicker polymer shell-layer comparing to the corresponding seeds in Fig. 4B and D, respectively.

The successful incorporation of various functional groups, including hydroxyl and carboxyl, onto the polymer shell-layer of PE/$SiO_2$/polymer hybrid microspheres was further proven by FT-IR spectra in Fig. 4g and 4h, respectively. Both FT-IR spectra of PE/$SiO_2$/polymer hybrids had a strong peak at 1100 $cm^{-1}$ of the asymmetrical vibration of Si–O–Si bond of the silica mid-layer. The strong peak at 1728 $cm^{-1}$ in Fig. 4g was assigned to the stretching vibration of the carbonyl unit of ester group of PHEMA component, confirming the formation of PE/$SiO_2$/P(MBAAm-*co*-HEMA) hybrid microspheres. The presence of a strong peak at 1700 $cm^{-1}$ in Fig. 2h was ascribed to the stretching vibration of the carbonyl unit of the carboxyl group of PMAA component, indicating that P(MBAAm-*co*-MAA) shell-layer was encapsulated over MPS-modified PE/$SiO_2$ seeds.

All the TEM micrographs in Fig. 4 indicated that the resultant PE/$SiO_2$/polymer hybrid microspheres with different functional groups, including amide, hydroxyl, and carboxyl, had smooth and non-segmented surfaces without formation of any secondary-initiated particles, which demonstrated that the vinyl groups on the surface of MPS-modified PE/$SiO_2$ seeds had enough capture ability of the radical species during the forth-stage distillation precipitation polymerization as shown in Scheme 1.

The experimental conditions for the forth-stage distillation precipitation polymerization of functional comonomers, including NIPAAm, HEMA and MAA, respectively, together with MBAAm as a crosslinker in presence of MPS-modified PE/$SiO_2$ particles as seeds, size and size distribution of the resultant functional PE/$SiO_2$/polymer hybrid microspheres were summarized in Table 2. The size of the PE/$SiO_2$/polymer hybrid microspheres varied between 463 and 484 nm, which depended on the type of functional comonomer used for the copolymerizations. The maximum diameter of 484 nm and minimum diameter of 463 nm were afforded with PE/$SiO_2$/P(MBAAm-*co*-NIPAAm) (Entry A) and PE/$SiO_2$/P(MBAAm-*co*-MAA) (Entry C), respectively, which may be due to the different reactivity of the comonomers of NIPAAm, HEMA, and MAA during the copolymerizations. All the diameters of the resultant PE/$SiO_2$/polymer functional hybrid microspheres were significantly larger than that of the MPS-modified PE/$SiO_2$ seeds (404 nm). These results meant that the thickness of (MBAAm-*co*-NIPAAm) with amide group (40 nm), P(MBAAm-*co*-HEMA) with hydroxyl group (33 nm) and P(MBAAm-*co*-MAA) (30 nm) with carboxyl were successfully formed as the shell-layer of the resultant tetra-layer

**Table 2**
Reaction conditions, size, size distribution, and shell thickness of PE/$SiO_2$/polymer tetra-layer microspheres with various functional groups on the shell-layer.

| Entry | Seed (g) | MBAAM (g) | Comonomer | Dn (nm) | Dw (nm) | U | Thickness of outer layer[c](nm) |
|---|---|---|---|---|---|---|---|
| A[a] | 0.1 | 0.06 | NIPAAm 0.09 g | 484/556[d] | 487 | 1.006/1.007[d] | 40 |
| B[a] | 0.1 | 0.06 | HEMA 0.09 mL | 471 | 473 | 1.004 | 33.5 |
| C[b] | 0.1 | 0.06 | HEMA 0.09 mL | 526/574[d] | 530 | 1.008/1.005[d] | 61 |
| D[a] | 0.1 | 0.06 | MAA 0.09 mL | 463 | 466 | 1.006 | 29.5 |
| E[b] | 0.1 | 0.06 | MAA 0.09 mL | 516/547[d] | 518 | 1.004/1.002[d] | 56 |

(A) PE/$SiO_2$/P(MBAAm-co-NIPAAm); (B) PE/$SiO_2$/P(MBAAm-*co*-HEMA) after first-semibatch polymerization; (C) PE/$SiO_2$/P(MBAAm-*co*-HEMA) after second semibatch polymerization; (D) PE/$SiO_2$/P(MBAAm-*co*-MAA) after first-semibatch polymerization; (E) PE/$SiO_2$/P(MBAAm-*co*-MAA) after second semibatch polymerization.

[a] One-layer polymer shell encapsulated onto the quaternary ammonium /Silica

[b] Two-layer polymer shell encapsulated onto the quaternary ammonium /Silica

[c] Shell thickness = $(D_{core-shell}-D_{seed})/2$ in TEM micrographs

[d] Hydrodynamic diameter and polydispersity index of the hollow polymer microspheres from DLS

PE/$SiO_2$/polymer hybrid microspheres via the forth-stage distillation precipitation polymerization. All the polydispersity indexes ($U$) of the resultant PE/$SiO_2$/polymer hybrid microspheres were maintained between 1.004 and 1.006, indicating that the hybrid microspheres were monodispersed.

The sizes of PE/$SiO_2$/P(MBAAm-*co*-HEMA) and PE/$SiO_2$/P(MBAAm-*co*-MAA) were listed in Table 2 by the two-semibatch mode distillation precipitation polymerization, which indicated that the diameters of the hybrid microspheres were considerably enlarged from 471 nm (Entry B) to 526 nm (Entry C) and from 463 nm (Entry D) to 516 nm (Entry E), respectively. In such a way, the monodisperse PE/$SiO_2$/polymer hybrid microspheres with different thicknesses (ranging from 30 to 61 nm in the present work as summarized in Table 2) can be well controlled via the multi-semibatch mode distillation precipitation polymerization by successive introducing AIBN initiator and the designed amount of MBAAm crosslinker and the corresponding comonomers into the polymerization system.

### *3.4. Synthesis of monodisperse hollow polymer microspheres with movable PE cores and various functional group on the shell-layer*

The sandwiched silica-layer of the PE/$SiO_2$/polymer hybrid microspheres can be selectively removed by etching in hydrofluoric acid (HF) to afford the corresponding hollow polymer microspheres with movable PE core and various functional groups on the shell-layer. The driving force for such selective removal was originated from the formation of $SiF_4$ gas, which was given off from the hybrid microspheres during the etching process. Typical TEM micrographs of hollow (MBAAm-*co*-NIPAAm), (MBAAm-*co*-HEMA) and (MBAAm-*co*-MAA) microspheres with movable PE cores were illustrated in Fig. 5A–C, respectively, which were developed by the selective removal of silica mid-layer from the corresponding PE/$SiO_2$/polymer hybrid microspheres as shown in Fig. 4A, C, and E. All the TEM micrographs of hollow functional polymer microspheres had convincing hollow-sphere structures in the presence of circular rings with sectioned spheres and a cavity in the mid-layer of the microspheres, in which all the PE cores were not located in the centers of these hollow microspheres any more. The size and shape of these colloids were essentially unchanged during HF etching process, and the functional polymer shells did not collapse when liquid was evaporated from their interior during the TEM sample preparation. All these results implied that the polymer shell with different functional groups was thick enough to support the hollow structure in the present work. It was believed that the encapsulated PE cores were free to move with the functional polymer shell if the hollow microspheres were filled with liquid. After the liquids were completely evaporated, the PE cores tended to stick to the walls as a result of the attractive capillary force between the surfaces of the PE core and polymer shell-layer, which was much similar to the results reported in the literature [14–25].

The hydrodynamic size and size distribution of the resultant hollow polymer microspheres with movable PE cores were determined using DLS in water for comparison to the results from TEM characterization (only with three samples for comparison as Entries A, C and E in Table 2). The hydrodynamic diameters of hollow (MBAAm-*co*-NIPAAm), (MBAAm-*co*-HEMA) and (MBAAm-*co*-MAA)

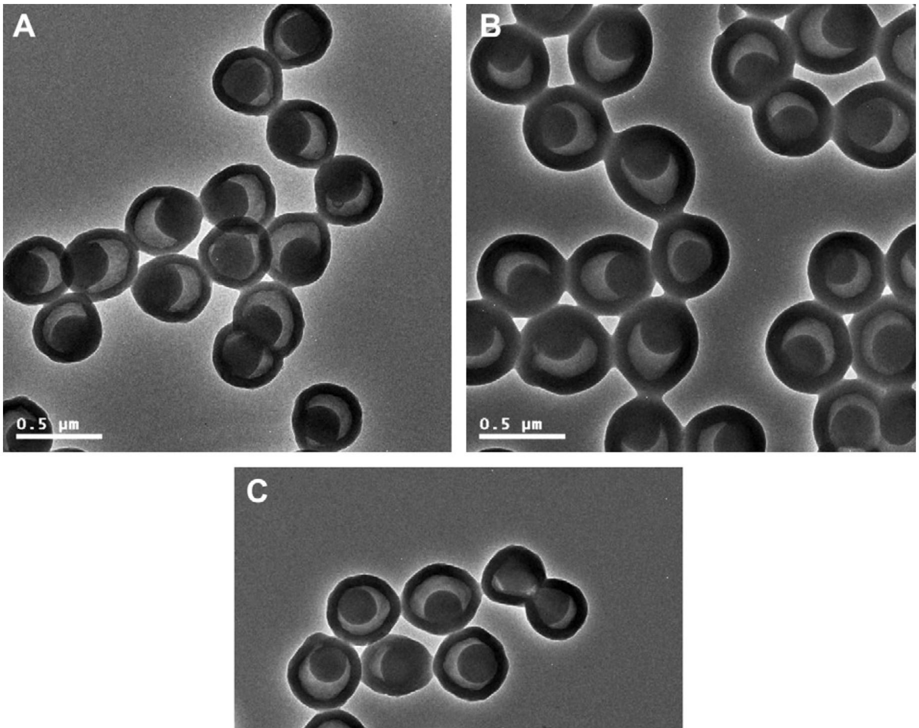

**Fig. 5.** TEM micrographs of hollow polymer microspheres containing movable pyridinium PE cores with various functional groups on the shell-layer: (A) P(MBAAm-*co*-NIPAAm); (B) P(MBAAm-*co*-HEMA); (C) P(MBAAm-*co*-MAA).

microspheres with movable PE cores were 556, 574 and 547 nm with monodispersity indexes (*U*) of 1.007, 1.005 and 1.002, respectively. The considerable larger hydrodynamic diameters (556, 574 and 547 nm) of the hollow microspheres than the corresponding sizes from TEM observation (484, 526 and 516 nm) confirmed the hydrophilic property of the resultant hollow polymer microspheres with movable PE cores and various functional groups on the polymer shell-layer, including amide, hydroxyl and carboxyl, as the former diameters were obtained from a swelling state in water. The hydrophilicity, functionality on the polymer shell-layer of the hollow polymer microspheres containing movable cationic PE core will enable them as potential materials for drug protection and delivery system, bio-separation and bio-analysis. The study on the scope of this technique, including the extension to the other hollow structure particles and the application of such functional hollow microspheres with movable cores, is in progress.

## 4. Conclusion

Hollow (MBAAm-*co*-NIPAAm), (MBAAm-*co*-HEMA) and (MBAAm-*co*-MAA) microspheres with amide, hydroxyl and carboxyl groups on the polymer shell-layer containing movable cationic P(EGDMA-*co*-MAA)@P(EGDMA-*co*-VPyBzCl) polyelectrolyte (PE) cores were prepared by a facile route with a four-stage reaction and subsequent removal of the sandwiched silica-layer from the corresponding PE/$SiO_2$/polymer hybrid microspheres in hydrofluoric acid. The tetra-layer hybrids were synthesized by the combination of distillation precipitation polymerization for the formation of polymer core and polymer shell-layer, and the controlled hydrolysis of TEOS in ethanol/water mixed solvent via a modified Stöber process. The efficient electrostatic interaction between the cationic charges on the surface of PE cores and the negative siliceous species was essential to afford monodisperse PE/$SiO_2$ composites during the controlled hydrolysis of TEOS. The polymer shell-layer with various functional groups were successfully encapsulated onto the MPS-modified PE/$SiO_2$ seeds, during which the capture ability of the incorporated vinyl groups for the newly formed radical species and comonomers played a key role for the construction of the final monodisperse PE/$SiO_2$/polymer hybrid microspheres with a tetra-layer structure. Further, the thickness of the functional polymer shell-layer can be well controlled by a multi-semibatch distillation precipitation polymerization mode.

## Acknowledgements

This work was supported by the National Science Foundation of China with Project No. of 20874049.

## References

[1] Caruso F. Adv Mater 2001;13:11.
[2] Gill I, Ballesteros A. J Am Chem Soc 2004;126:7908.
[3] Zhang J, Xu S, Kumacheva E. J Am Chem Soc 2004;126:7908.
[4] McDonald CJ, Blouck KJ, Chaupt AB, Stevens CJ. Macromolecules 2000;33: 1593.
[5] Li GL, Yang XY, Wang B, Wang JY, Yang XL. Polymer 2008;49:3436.
[6] Park MK, Onishi K, Locklin J, Caruso F, Advincula RC. Langmuir 2003;19: 8550.
[7] Stewart S, Liu GJ. Chem Mater 1999;11:1048.
[8] Mandal TK, Fleming MS, Walt DR. Chem Mater 2000;12:3481.
[9] Toshiaki D, Furukawa T, Narita T, Shimofure S. Langmuir 2001;17:4525–8.
[10] Su QH, Deng YL. J Am Chem Soc 2005;127:8274–5.
[11] Donath E, Sukhorukov GB, Caruso F, Davis SA, MÖhwald H. Angew Chem Int Ed 1998;37:2201–5.
[12] Déjugnat C, Sukhorukov GB. Langmuir 2004;20:7265–9.
[13] Peyratout CS, Dähne L. Angew Chem Int Ed 2004;43:3762–83.
[14] Kamata K, Lu Y, Xia YN. J Am Chem Soc 2003;125:2384.
[15] Kim M, Sohn K, Na HB, Hyeon T. Nano Lett 2002;2:1383.
[16] Cheng DM, Zhou XD, Xia HB, Chan HSO. Chem Mater 2005;17:3578.
[17] Lee KT, Jung YS, Oh SM. J Am Chem Soc 2003;125:5652.
[18] Zhang K, Zhang XH, Chen HT, Chen X, Zhang LL, Zhang JH, et al. Langmuir 2004;20:11312.
[19] Li GL, Liu G, Kang ET, Neoh KG, Yang XL. Langmuir 2008;24:9050.
[20] Li GL, Yang XL. J Phys Chem B 2007;111:12781.
[21] Ji HF, Wang SP, Yang XL. Polymer 2009;50:133.
[22] Zhang TH, Pang JB, Tan G, He JB, McPherson GL, Lu YF, et al. Langmuir 2007;23:5143.
[23] Liu GY, Yang XL, Wang YM. Langmuir 2008;24:5485.
[24] Liu GY, Wang H, Yang XL. Polymer 2009;50:2578.
[25] Sun ZC, Bai F, Wu HM, Schmitt SK, Baye DM, Fan HY. J Am Chem Soc 2009;131:13594–5.
[26] Hah HJ, Um JI, Han SH, Koo SM. Chem Comm 2004:1012.
[27] Liu W, Yang XL, He XG. Chin J Polym Sci 2009;27:275.
[28] Shiga K, Muramatsu N, Kondo. J Pharm Pharmacol 1996;48:491.
[29] Chattopadhyay P, Shakunov BY, Yim D, Cipolla D, Boyd B, Farr S. Adv Drug Deliv Rev 2007;59:444.
[30] Schönhoff MJ. Phys Condens Matter 2003;15:R1781.
[31] Bertrand P, Jonas A, Laschewsky A, Legras R. Macromol Rapid Commun 2000;21:319.
[32] Decher G. Science 1997;277:1232.
[33] Fabianowski W, Roszko M, Brodzinska W. Thin Solid Films 1998;327–329: 743.
[34] Liu GY, Yang XL, Wang YM. Polymer 2007;48:4385.
[35] Liu GY, Zhang H, Yang XL, Wang YM. Polymer 2007;48:5896.
[36] Liu GY, Li LY, Yang XL, Dai Z. Polym Adv Technol 2008;19:1922.
[37] Liu GY, Zhang H, Yang XL, Wang YM. J Appl Polym Sci 2009;111:1964.
[38] Bai F, Yang XL, Li R, Huang B, Huang WQ. Polymer 2006;47:5775.
[39] Wang JY, Yang XL. Langmuir 2008;24:3358.
[40] Bai F, Huang B, Yang XL, Huang WQ. Eur Polym J 2007;43:3923.
[41] Yuan JJ, Mykhaylyk OO, Ryan AJ, Armes SP. J Am Chem Soc 2007;129:1717.
[42] Lu Y, McLellan J, Xia YN. Langmuir 2004;20:3464.
[43] Chen M, Zhou XS, Wu LM, Xie SH, Chen Y. Macromol Chem Phys 2005;206: 1896.
[44] Wang JY, Yang XL. Colloid Polym Sci 2008;286:283.
[45] Bai F, Yang XL, Huang WQ. Macromolecules 2004;37:9746.
[46] Bourgeat-Lami E, Lang J. J Colloid Interface Sci 1998;197:293.
[47] Prokopov NI, Gritskova IA, Charkasov VR, Chalykh AE. Russ Chem Rev 1996;65:167.
[48] Kawaguchi H. Prog Polym Sci 2000;25:1171.